Original Scientific Paper

Journal of Applied Engineering Science

doi:10.5937/jaes17-22408

Paper number: 17(2019)3, 624, 413 - 424

DEVELOPMENT AND EXPERIMENTAL VERIFICATION OF THE MATHEMATICAL MODEL OF THERMAL INERTIA FOR A BRANCHED HEAT SUPPLY SYSTEM

Andrey Batukhtin, Irina Batukhtina, Maxim Bass*, Sergey Batukhtin, Mihail Kobylkin, Marina Baranovskaya, Alena Baranovskaya

Transbaikal state university, Russian Federation

The article describes a new method for making management decisions on heat supply in district heating systems, based on solving a sequence of recurrence relations of first-order differential equations, enabling to synthesize daily schedules of heat supply in such systems. Using first order differential equations, we implement real-time daily heat supply scheduling, predict the time-temperature dependence for heating water in the supply line, and we form a decision on the thermal energy delivery on the basis of this information. The effectiveness of our method is confirmed by numerical modeling and comparative analysis of daily heat supply scheduling with the help of advanced intelligent decision making tools. For comparative analysis, we considered daily scheduling using a nonlinear regression model, a generalized regression neural network, a radial basis neural network, and a linear neural network. The effectiveness of our method was estimated on the basis of MAPE (mean absolute percentage error) and Accuracy coefficients. The model was recognized as most effective for which the MAPE value was maximum, and the Accuracy value tended to one hundred percent. Experimental studies showed that our proposed model has an advantage over the regression model by 1.68 times and over the neural models by more than 10.2 times when modeling for a hundred heating network sections. Thus, the main purpose of our study was to increase the accuracy of the method of making a managerial heat supply decision based on the experimental verification of a mathematical model of thermal inertia of a branched district heating system.

Keywords: district heating systems, first-order differential equations, regression, generalized regression neural network, radial basis neural network, linear neural network, accuracy, inertia, mathematical models, scheduling

INTRODUCTION

The problem of mathematical support for daily heat supply scheduling in district heating systems (DHS) in the Russian Federation began to take shape in the 1950s. Professor E.Ya. Sokolov [1], a leading scholar in this field, theoretically substantiated the methods for heat supply scheduling. The current state of the DHS is characterized by significant uneven daily consumption. This is caused by a sharp decrease in industrial consumption, increased comfort of housing under construction (an increase in the share of hot water supply), increased share of consumers equipped with sophisticated automatic control systems and the widespread introduction of commercial heat metering (due to the amendments in the regulatory framework).

The irregularity of the daily heat consumption in the DHS requires introducing thermal energy regulation during the day – the daily heat control. Currently, the problem of constructing a thermal inertia model for district heating networks has been solved under the condition of averaging the characteristics of branched heating networks and representing the system as a single pipeline. Experimental verification of this model at a number of DHSs of the Trans-Baikal Territory in the Russian Federation showed that its operability only for similar sections in case of insignificant temperature perturbations. Since modern DHSs differ in a significant branching, length, and have different thermophysical properties at different sites, the use of averaged characteristics introduces significant errors in the model. Therefore, the problem of daily heat supply scheduling is associated with an insufficient amount of research in the field of algorithmization and intellectualization of the managerial decision making process concerning heat supply. In general, the current state of mathematical and algorithmic support for daily heat supply scheduling in the DHS is characterized by the absence of ready-made algorithms that take into account the real thermophysical properties of heating networks and enclosing structures, as well as their operating characteristics [1, 2].

These algorithms should reflect the thermal inertia of heating networks with regard to their thermophysical properties, branching and hydraulic modes. In addition, these mathematical models should take into account the heat-accumulating properties of heat consumers [3].

In general terms, thermal inertia models of heating networks have been solved only in a simplified form: without regard to losses due to thermal insulation, degree of branching and characteristics of the hydraulic modes at the heating network sections. A whole class of engineering and economic tasks (heat engineering, transport, information, technical and economic optimization, etc.) can be reduced to a sequence of recurrent relations of

*mbass77@yandex.ru

first order differential equations with a linear dependence in the right-hand side. Such tasks include thermodynamic analysis models [4-11], heat and power system models [12–16], combustion models [17– 22], models of local heat exchange systems (for example, solar collectors [23–28]), and others.

Nowadays, systems of homogeneous and inhomogeneous differential equations are one of the main tools for mathematical modeling of physical processes [14]. In [15], a system of homogeneous differential equations for controlling adsorption chillers is discussed. The solution is considered by gradient steps and is not represented as a direct analytical dependence. Richard Kicsiny considers modern mathematical models for heating systems with pipes based on the differential equations of Newton's law for cooling a pipe in a number of recent papers [14, 16]. A fairly common task to improve the efficiency of urban heating networks is to build their dynamic models. They are based, as a rule, on systems of differential equations, and their solution is reduced either to numerical solutions [29, 30], or to a significant simplification of the model and considering it through one or two equations for average parameters, solved by known dependencies [31].

Systems of homogeneous and inhomogeneous differential equations underlie the theory describing the combustion processes. For example, when constructing reliable mathematical models for the gasification of solid fuel particles, systems with hundreds of differential equations are compiled [32]. As a rule, these systems are reduced by the finite difference method to ordinary equations, which leads to a relative loss of accuracy and the absence of direct analytical solutions [19].

The worldwide growing use of alternative and renewable energy sources has formed a separate direction in the theory of mathematical modeling concerning solar collectors. As a rule, their modeling is reduced to solving systems and individual differential equations. For example, the multiple linear regression method was improved for solving differential equations simulating a solar collector in [29]. A numerical and experimental study of a flat solar collector is presented in [23], where hydrodynamics and heat transfer in the collector panel are determined by transforming differential equations by the finite difference method. A mathematical model described in [33] is used for simulating transient processes that occur in a heated flat collector fluid. The model is based on solving a system of coupled differential equations describing the thermal processes of glazing, air gap, fluid, etc. The system of differential equations is solved iteratively in the MATLAB program. Most of the modeling problems are reduced to the numerical solution of systems of differential equations in this system [34] and similar ones. Such studies can be exemplified by modeling projects (based on numerical solutions) of hybrid solar photovoltaic-thermal systems [35-38], as well as by the projects on modeling the optimal strategy of heating control planning using green technologies based on wind energy [39].

Advanced intelligent tools for modeling daily distribution schedules include neural networks based on various control signal generation algorithms, such as described in [40, 41]. The main disadvantages of the known approaches in solving systems of differential equations in applied intellectual problems of physical process simulation are the limited accuracy of the solution and the high requirements for computational tools implementing them for multidimensional systems, as well as a limited possibility of using the solutions obtained in more complex models. One of the solutions to this problem is to develop a direct analytical solution on heat supply in district heating systems, which is presented in the second section of this article.

METHODOLOGY

Obtaining a general solution for a sequence of recurrence relations

The sequence of recurrence relations of the first-order differential equations with a linear dependence in the right part is written as:

$$\begin{cases} y_1' = A_1 \cdot y_1 + (\alpha_1 \cdot y_0 + \beta_1); \\ y_2' = A_2 \cdot y_2 + (\alpha_2 \cdot y_1 + \beta_2); \\ y_3' = A_3 \cdot y_3 + (\alpha_3 \cdot y_2 + \beta_3); \\ \ldots\ldots\ldots\ldots\ldots\ldots\ldots\ldots\ldots \\ y_N' = A_N \cdot y_N + (\alpha_N \cdot y_{(N-1)} + \beta_N); \end{cases} \quad (1)$$

where $A_1,\ldots,A_N$, $\alpha_1,\ldots,\alpha_N$, $\beta_1,\ldots,\beta_N$ are constants;

$y_1',\ldots,y_N'$, $\frac{dy_1}{dx},\ldots,\frac{dy_N}{dx}$ – first derivatives, respectively.

A partial solution to the system (1) is usually conditioned by a sequence of initial distributions of parameter $y_1,\ldots,y_N$ at $x=0$:

$$x = 0 \Rightarrow y_1 = y_1^H \ldots y_N = y_N^H \quad (2)$$

The sequence of recurrence relations is a solution to the system of differential equations (1):

$$y_1 = e^{A_1 \cdot x} \cdot \left[y_1^H - \int e^{-A_1 \cdot x} \cdot (\alpha_1 \cdot y_0 + \beta_1) \cdot dx \Big|_{x=0} + \int e^{-A_1 \cdot x} \cdot (\alpha_1 \cdot y_0 + \beta_1) \cdot dx \right]$$

$$y_N = e^{A_N \cdot x} \cdot \left[y_N^H - \int e^{-A_N \cdot x} \cdot (\alpha_N \cdot y_{(N-1)} + \beta_N) \cdot dx \Big|_{x=0} + \int e^{-A_N \cdot x} \cdot (\alpha_N \cdot y_{(N-1)} + \beta_N) \cdot dx \right] \quad (3)$$

It is convenient to represent the general solution as:

$$y_N = e^{A_N \cdot x} \cdot y_N^H + \sum_{S=0}^{N-1} \left[\left(e^{A_S \cdot x} - e^{A_N \cdot x} \right) \cdot \gamma_S^P \right] \quad (4)$$

where γ_S^P – a system of products of predefined constants A_1 ... A_N, α_1 ... α_N, β_1 ... β_N, S1…SN, P1…PN and initial conditions.

To determine the general solution (4) γ_S^P for three components:

$$\gamma_S^N = \gamma_S^N(y_0) + \gamma_S^N(y^H) + \gamma_S^N(\beta) \quad (5)$$

Components γ_S^P can be determined as:

$$\gamma_S^N(y_0) = y_0 \cdot \left(\psi_{\Pi P=0}^{S(-)} \cdot \prod_{R=S+1}^{N} \left[\frac{1}{A_S - A_R} \cdot \alpha_R \right] \right) \quad (6)$$

$$\gamma_S^N(\beta) = \sum_{I=1}^{S} \left[\frac{\beta_I}{\alpha_I} \cdot \psi_{n P=I-1}^{S(-)} \cdot \prod_{R=S+1}^{N} \left(\frac{1}{A_S - A_R} \cdot \alpha_R \right) \right] \quad (7)$$

$$\gamma_S^N(y^H) = \sum_{I=1}^{S} \left[y_I^H \cdot \psi_{\Pi P=I}^{S(-)} \cdot \prod_{R=S+1}^{N} \left(\frac{1}{A_S - A_R} \cdot \alpha_R \right) \right] \quad (8)$$

With regard to (6-8) we will write down the solution to the initial system (1):

$$y_N = e^{A_N \cdot x} \cdot y_N^H + \sum_{S=0}^{N-1} \left[\left(e^{A_S \cdot x} - e^{A_N \cdot x} \right) \cdot \left(\gamma_S^N(y_0) + \gamma_S^N(y^H) + \gamma_S^N(\beta) \right) \right] \quad (9)$$

The values of the components Ψ can be obtained by recurrent substitution with sequential integration according to the methodology of [38].

It should be noted that the values of the components γ_S^P are a special case at *S=0:*

$$\gamma_0^N(y_0) = y_0 \cdot \prod_{I=1}^{N} \left(\frac{1}{A_0 - A_I} \cdot \alpha_I \right) \quad (10)$$

$$\gamma_0^N(\beta) = \sum_{I=1}^{S} \left[\frac{\beta_I}{\alpha_I} \cdot \prod_{R=I}^{N} \left(\frac{1}{A_0 - A_R} \cdot \alpha_R \right) \right] \quad (11)$$

$$\gamma_0^N(y^H) = 0 \quad (12)$$

Development of a mathematical model of thermal inertia for a branched heating system based on solving a sequence of recurrence relations of the first-order differential equations

The heat balance of the network water flow at the end of the heating network section with temperature perturbation at its beginning can be written in the following form:

$$V_1 \cdot c_P \cdot \rho_w \cdot dt_1 = -\upsilon_1 \cdot c_P \cdot \rho_w \cdot \left(t_1 - t_1^y \right) \cdot d\tau \quad (13)$$

where:

c_p – heat capacity of the network water, kJ/kg•°C;

ρ_m – density of the network water, kg/m³;

t_1 – water temperature at the end of the heating network section at time $d\tau$, °C;

t_1^y – water temperature at the end of the heating network section at time $\tau \to \infty$, °C;

V_1 – volume of the heating network section, m³;

υ_1 – volumetric water discharge at the section, m³/s.

Heat losses in the considered area can be accounted for by writing the steady state heat balance equation:

$$\left(t_0 - t_1^y \right) \cdot \upsilon_1 \cdot c_P \cdot \rho_w = K_1 \cdot \pi \cdot l_1 \cdot \left(1 + \mu_1 \right) \cdot \left(\bar{t}_1^y - t_n \right) \quad (14)$$

where: t_0 – temperature perturbation at the beginning of the heating network section, °C;

t_1^{-y} – average temperature of the network water at the heating network section, °C;

υ_1 – volumetric water discharge at the section, m³/s.

μ_1 – local heat loss coefficient of the heating network section;

$K_1 \bullet \pi$ – linear heat losses;

l_1 – pipeline length of the heating network section, m.

Solving equation (14) concerning t_1^y with respect to the fact that $\bar{t}_1^y = \frac{t_1^y + t_0}{2}$, we get the following:

$$t_1^y = t_0 \cdot \frac{2 - \varepsilon_{TN1}}{2 + \varepsilon_{TN1}} + 2 \cdot t_n \cdot \frac{\varepsilon_{TN1}}{2 + \varepsilon_{TN1}} \quad (15)$$

where $\varepsilon_{TN1} = \frac{K_1 \cdot \pi \cdot l_1 \cdot (1 + \mu_1)}{\upsilon_1 \cdot c_P \cdot \rho_w}$ is a dimensionless comple that characterizes the ratio of heat loss through the thermal insulation of the heating network section to the water flow passing through it.

In view of (15), equation (13) can be written as:

$$V_1 \cdot c_P \cdot \rho_w \cdot dt_1 = -\upsilon_1 \cdot c_P \cdot \rho_w \cdot \left(t_1 - t_0 \cdot \frac{2 - \varepsilon_{TN1}}{2 + \varepsilon_{TN1}} - 2 \cdot t_n \cdot \frac{\varepsilon_{TN1}}{2 + \varepsilon_{TN1}} \right) \cdot d\tau \quad (16)$$

Or it can be written in the form of a homogeneous first-order differential equation:

$$\begin{cases} q_1 \cdot t_1' = f_1 \cdot t_1 + \phi_1 \\ \phi_1 = -\left(t_0 \cdot \frac{2 - \varepsilon_{TN1}}{2 + \varepsilon_{TN1}} + 2 \cdot t_n \cdot \frac{\varepsilon_{TN1}}{2 + \varepsilon_{TN1}} \right) \\ f_1 = 1 \\ q_1 = -\frac{1}{\varphi_1} \end{cases} \quad (17)$$

where: $\varphi_1 = \frac{\upsilon_1}{V_1}$ – relative consumption of heating water at the heating network section.

The solution to equation (17) is written as follows:

$$t_1 = t_0 \cdot \frac{2 - \varepsilon_{TN1}}{2 + \varepsilon_{TN1}} \cdot \left(1 - e^{-\varphi_1 \cdot \tau} \right) + t_1^n \cdot e^{-\varphi_1 \cdot \tau} + 2 \cdot t_n \cdot \frac{\varepsilon_{TN1}}{2 + \varepsilon_{TN1}} \cdot \left(1 - e^{-\varphi_1 \cdot \tau} \right) \quad (18)$$

To simulate an unsteady temperature condition of heating networks, taking into account their heat-accumulating properties and a multivariate configuration, it is necessary to consider the temperature condition of a complex of consecutive sections from the heat supply source to a specific consumer. Let us consider an approximate solution to this problem through the averaged parameters of the heating network. To do this it is required to get a solution in the form of $t_{nTN} = f(t_0, \tau)$ to equation

$$\sum_{i=1}^{n_{TN}} \frac{1}{\varphi_i} \cdot dt_{n_{TN}} = -\left(t_{n_{TN}} - t^{y}_{n_{TN}}\right) \cdot d\tau \tag{19}$$

Value of t^{y}_{nTN} can be found from the solution of the system of auxiliary balances:

$$\begin{cases} \left(t_0 - t_1^y\right) \cdot \upsilon_1 \cdot c_P \cdot \rho_w = K_1 \cdot \pi \cdot l_1 \cdot \left(1 + \mu_1\right) \cdot \left(\bar{t}_1^{\,y} - t_n\right) \\ \left(t_1 - t_2^y\right) \cdot \upsilon_2 \cdot c_P \cdot \rho_w = K_2 \cdot \pi \cdot l_2 \cdot \left(1 + \mu_2\right) \cdot \left(\bar{t}_2^{\,y} - t_n\right) \\ \ldots\ldots\ldots\ldots\ldots\ldots\ldots\ldots\ldots\ldots\ldots\ldots\ldots\ldots \\ \left(t_{n_{TN}-1} - t^{y}_{n_{TN}}\right) \cdot \upsilon_{n_{TN}} \cdot c_P \cdot \rho_w = K_{n_{TN}} \cdot \pi \cdot l_{n_{TN}} \\ \qquad \cdot \left(1 + \mu_{n_{TN}}\right) \cdot \left(\bar{t}^{\,y}_{n_{TN}} - t_n\right) \end{cases} \tag{20}$$

System (20) is transformed with regard to the transition to a dimensionless complex:

$$\begin{cases} \left(t_0 - t_1^y\right) = \varepsilon_{TN(1)} \cdot \left(\bar{t}_1^{\,y} - t_n\right) \\ \left(t_1 - t_2^y\right) = \varepsilon_{TN(2)} \cdot \left(\bar{t}_2^{\,y} - t_n\right) \\ \ldots\ldots\ldots\ldots\ldots\ldots\ldots\ldots\ldots\ldots \\ \left(t_{n_{TC}-1} - t^{y}_{n_{TC}}\right) = \varepsilon_{TN(n_{TC})} \cdot \left(\bar{t}^{\,y}_{n_{TC}} - t_n\right) \end{cases} \tag{21}$$

System (21) is transformed into the recurrence relation:

$$\begin{cases} t_1^y = t_0 \cdot \dfrac{2 - \varepsilon_{TN(1)}}{2 + \varepsilon_{TN(1)}} + 2 \cdot t_n \cdot \dfrac{\varepsilon_{TN(1)}}{2 + \varepsilon_{TN(1)}} \\ t_2^y = t_1^y \cdot \dfrac{2 - \varepsilon_{TN(2)}}{2 + \varepsilon_{TN(2)}} + 2 \cdot t_n \cdot \dfrac{\varepsilon_{TN(2)}}{2 + \varepsilon_{TN(2)}} \\ \ldots\ldots\ldots\ldots\ldots\ldots\ldots\ldots\ldots\ldots\ldots\ldots \\ t^{y}_{n_{TN}} = t^{y}_{n_{TN}^{-1}} \cdot \dfrac{2 - \varepsilon_{TN(n_{TN})}}{2 + \varepsilon_{TN(n_{TN})}} + 2 \cdot t_n \cdot \dfrac{\varepsilon_{TN(n_{TN})}}{2 + \varepsilon_{TN(n_{TN})}} \end{cases} \tag{22}$$

Solution to relation (22) was obtained as follows:

$$t_{n_{TN}} = t^{n}_{n_{TN}} \cdot \exp\left(-\frac{1}{\sum_{i=1}^{n_{TN}} \frac{1}{\varphi_i}} \cdot \tau\right) + \left(1 - \exp\left(-\frac{1}{\sum_{i=1}^{n_{TN}} \frac{1}{\varphi_i}} \cdot \tau\right)\right) \cdot \left(t_0 \cdot \prod_{i=1}^{n_{TN}} \left[\frac{2 - \varepsilon_{TN(i)}}{2 + \varepsilon_{TN(i)}}\right]\right) +$$

$$+ \left(1 - \exp\left(-\frac{1}{\sum_{i=1}^{n_{TN}} \frac{1}{\varphi_i}} \cdot \tau\right)\right) \cdot \left(2 \cdot t_n \cdot \left(\sum_{i=1}^{n_{TN}-1} \prod_{j=i+1}^{n_{TN}} \left[\frac{2 - \varepsilon_{TN(j)}}{2 + \varepsilon_{TN(j)}} \cdot \frac{\varepsilon_{TN(i)}}{2 + \varepsilon_{TN(i)}}\right] + \frac{\varepsilon_{TN(n_{TN})}}{2 + \varepsilon_{TN(n_{TN})}}\right)\right) \tag{23}$$

The exact solution to the problem of modeling the unsteady temperature condition of heating networks, taking into account their heat-accumulating properties and the multivariate configuration (it is necessary to consider the temperature condition of a complex of consecutive sections from the heat supply source to a specific consumer) can be obtained by solving a recurrently related system n_{TN} of differential equations:

$$\begin{cases} q_1 \cdot t_1' = f_1 \cdot t_1 + \phi_1(t_0) \\ q_2 \cdot t_2' = f_2 \cdot t_2 + \phi_2(t_1) \\ \ldots\ldots\ldots\ldots\ldots\ldots\ldots\ldots\ldots\ldots \\ q_{n_{TN}} \cdot t'_{n_{TN}} = f_{n_{TN}} \cdot t_{n_{TN}} + \phi_{n_{TN}}(t_{n_{TN}-1}) \end{cases} \tag{24}$$

where

$$\begin{cases} \phi_1(t_0) = -\left(t_0 \cdot \dfrac{2 - \varepsilon_{TN(1)}}{2 + \varepsilon_{TN(1)}} + 2 \cdot t_n \cdot \dfrac{\varepsilon_{TN(1)}}{2 + \varepsilon_{TN(1)}}\right) \\ \phi_2(t_1) = -\left(t_1 \cdot \dfrac{2 - \varepsilon_{TN(2)}}{2 + \varepsilon_{TN(2)}} + 2 \cdot t_n \cdot \dfrac{\varepsilon_{TN(2)}}{2 + \varepsilon_{TN(2)}}\right) \\ \ldots\ldots\ldots\ldots\ldots\ldots\ldots\ldots\ldots\ldots\ldots\ldots \\ \phi_{n_{TN}}(t_{n_{TN}-1}) = -\left(t_{n_{TN}-1} \cdot \dfrac{2 - \varepsilon_{TN(n_{TN})}}{2 + \varepsilon_{TN(n_{TN})}} + 2 \cdot t_n \cdot \dfrac{\varepsilon_{TN(n_{TN})}}{2 + \varepsilon_{TN(n_{TN})}}\right) \end{cases} \tag{25}$$

$$f_1 = f_2 = \cdots = f_{n_{TN}} = 1 \tag{26}$$

$$\begin{cases} q_1 = -\dfrac{1}{\varphi_1} \\ q_2 = -\dfrac{1}{\varphi_2} \\ \ldots\ldots\ldots \\ q_{n_{TN}} = -\dfrac{1}{\varphi_{n_{TN}}} \end{cases} \tag{27}$$

In addition to system (22), the system of auxiliary heat balances is used.

$$\begin{cases} \left(t_0 - t_1^y\right) \cdot \upsilon_1 \cdot c_P \cdot \rho_w = K_1 \cdot \pi \cdot l_1 \cdot \left(1 + \beta_1\right) \cdot \left(\bar{t}_1^{\,y} - t_n\right) \\ \left(t_1 - t_2^y\right) \cdot \upsilon_2 \cdot c_P \cdot \rho_w = K_2 \cdot \pi \cdot l_2 \cdot \left(1 + \beta_2\right) \cdot \left(\bar{t}_2^{\,y} - t_n\right) \\ \ldots\ldots\ldots\ldots\ldots\ldots\ldots\ldots\ldots\ldots\ldots\ldots\ldots\ldots \\ \left(t_{n_{TN}-1} - t^{y}_{n_{TN}}\right) \cdot \upsilon_{n_{TN}} \cdot c_P \cdot \rho_w = K_{n_{TN}} \cdot \pi \cdot l_{n_{TN}} \cdot \left(1 + \beta_{n_{TN}}\right) \cdot \left(\bar{t}^{\,y}_{n_{TN}} - tn\right) \end{cases} \tag{28}$$

as well as the system of initial conditions:

$$\tau = 0 \rightarrow \begin{cases} t_1 = t_1^n \\ t_2 = t_2^n \\ \ldots\ldots \\ t_{n_{TN}} = t_{n_{TN}}^n \end{cases} \quad (29)$$

The general solution to system (22) can be written as follows:

$$t_{n_{TN}} = e^{A_{n_{TN}} \cdot \tau} \cdot t_{n_{TN}}^H + \sum_{S=0}^{n_{TN}-1} \left[\left(e^{A_S \cdot \tau} - e^{A_{n_{TN}} \cdot \tau} \right) \cdot \left(\gamma_S^{n_{TN}}(t_0) + \gamma_S^{n_{TN}}(t^H) + \gamma_S^{n_{TN}}(\beta) \right) \right] \quad (30)$$

where: at $S = 1, \ldots, n_{TN}-1$

$$\gamma_S^{n_{TN}}(t_0) = t_0 \cdot \left(\psi_{P=0}^{(-)S} \cdot \prod_{R=S+1}^{n_{TN}} \left[\frac{1}{A_S - A_R} \cdot \alpha_R \right] \right) \quad (31)$$

$$\gamma_S^{n_{TN}}(\beta) = \sum_{I=1}^{S} \left[\frac{\beta_I}{\alpha_I} \cdot \psi_{P=I-1}^{(-)S} \cdot \prod_{R=S+1}^{n_{TN}} \left(\frac{1}{A_S - A_R} \cdot \alpha_R \right) \right] \quad (32)$$

$$\gamma_S^{n_{TN}}(t^H) = \sum_{I=1}^{S} \left[t_I^H \cdot \psi_{P=I}^{(-)S} \cdot \prod_{R=S+1}^{n_{TN}} \left(\frac{1}{A_S - A_R} \cdot \alpha_R \right) \right] \quad (33)$$

at $S = 0$

$$\gamma_0^{n_{TN}}(t_0) = t_0 \cdot \prod_{I=1}^{n_{TN}} \left(\frac{1}{A_0 - A_I} \cdot \alpha_I \right) \quad (34)$$

$$\gamma_0^{n_{TN}}(\beta) = \sum_{I=1}^{S} \left[\frac{\beta_I}{\alpha_I} \cdot \prod_{R=I}^{n_{TN}} \left(\frac{1}{A_0 - A_R} \cdot \alpha_R \right) \right] \quad (35)$$

$$\gamma_0^{n_{TN}}(t^H) = 0 \quad (36)$$

$$\gamma_S^{n_{TN}} = \gamma_S^{n_{TN}}(t_0) + \gamma_S^{n_{TN}}(t^H) + \gamma_S^{n_{TN}}(\beta) \quad (37)$$

Taking into account the designation:

$$t_{n_{TC}} = e^{A_{n_{TN}} \cdot \tau} \cdot t_{n_{TN}}^H + \sum_{S=0}^{n_{TN}-1} \left[\left(e^{A_S \cdot \tau} - e^{A_{n_{TN}} \cdot \tau} \right) \cdot \gamma_S^{n_{TN}} \right] \quad (38)$$

The general solution to system (30) is convenient to represent as:

Equation (38) is used for daily heat supply scheduling, and in contrast to the well-known methods of solving systems of first-order differential equations, the direct analytical dependence (38) can be used in more complex models.

RESULTS

Description of the experimental research facility

Experimental verification of the mathematical model of thermal inertia for a district heat supply system was carried out in the framework of periodic tests for heat losses in the heating mains of the urban-type settlement of Yasnogorsk, the Trans-Baikal Region. A brief description of the test facility is given in Table 1.

Table 1: A brief description of the test facility

Description	Heating main	
	Supply line	Return line
1	2	3
Heating network scheme	Closed, dead-end line	Closed, dead-end line
Number of pipelines	1	1
Length, km	2.881	2.881
Nominal diameter (DN), mm	500.0; 400.0; 300.0	500.0; 400.0; 300.0
Type of pipeline laying at the section	above-ground pipelining on low supports and subsurface pipelining in crawlways	above-ground pipelining on low supports and subsurface pipelining in crawlways
Thermal insulation design	mineral wool mats	mineral wool mats
Year of pipeline laying	1990	1990
Heating schedule, ˚C	95 – 70	95 – 70
Temperature chart straightening for the needs of hot water supply, ˚C	60	60
Pipeline operation time, h	8520	8520
Pipeline repair period (month)	From AUG 15 through AUG 24	From AUG 15 through AUG 24
Heating season length	From AUG 25 through AUG 14	From AUG 25 through AUG 14

Journal of Applied Engineering Science Vol. 17, No. 3, 2019
ISSN 1451-4117

Heating water flow rate is measured in the test circuit using portable flow meters. The heating main characteristics are given in table 2.

Table 2: Heating main characteristics

Heating network section	Type of pipeline laying, thermal insulation design	Pipeline diameter			Pipeline length	Material characteristics	Cross-sectional area	Pipeline volume
		nominal	inner	outer				
		d_n, m	d_i, m	d_o, m	l, m	d_o*l, m^2	f, m^2	V, m^3
State District Power Plant (SDPP) - Booster Pumping Station	**above-ground;** mineral wool wired mats; safety blanket – glass cloth	0.500	0.510	0.530	1794.0	950.8	0.2043	366.48
BPS - HC-6 (Heating Chamber)	**subsurface;** glass wool and mineral wool mats; glass-reinforced plastic	0.400	0.406	0.426	565.0	240.7	0.1297	73.29
HC-6 - HC-12		0.300	0.315	0.325	522.0	169.7	0.0779	40.68
Total for above-ground pipeline laying					1794.0	950.8	---	366.5
Total for subsurface pipeline laying:					1087.0	410.3	---	114.0
Grand total for tested sites:633					2881.0	1361.2	---	480.5

A brief description of the tested network and the thermal preparation plant is shown in Fig. 1.

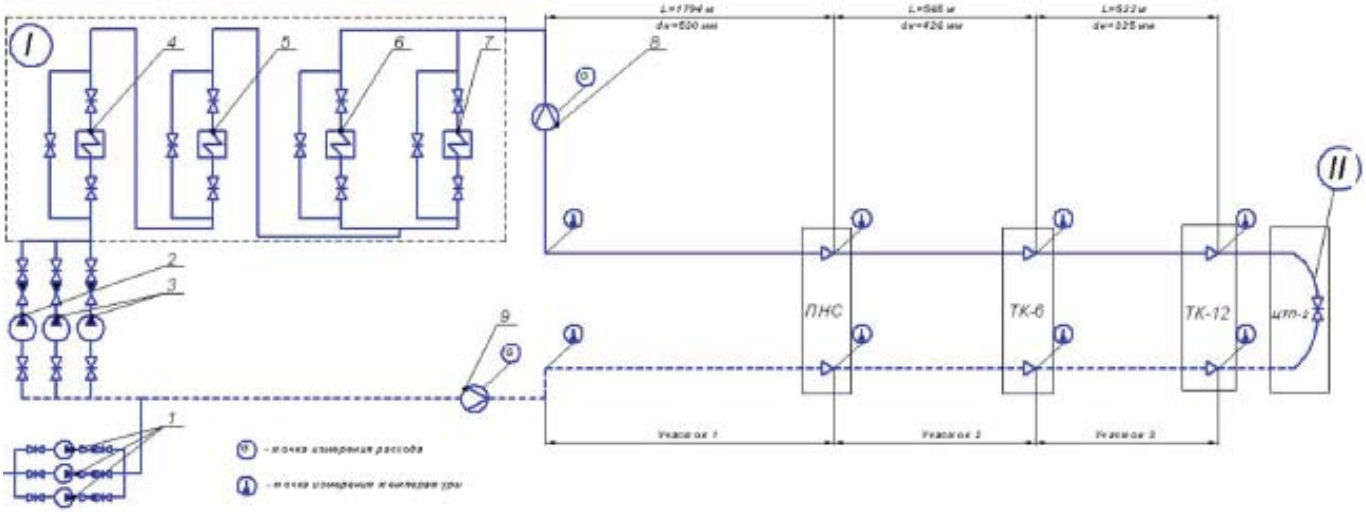

Figure 1: Schematic heating circuit,

where I – thermal preparation plant; II – circuit cross-connection; 1 – heating network makeup pumps; 2 – CP-400-210M circulation pulser; 3 –CP-400-210 circulation pulsers; 4 – MWH-1 main water heater; 5 – MWH-2; 6 – PWH-1 peak water heater; 7 – PWH-2; 8.9 – regular coolant flow rate control system

Test Preparation and Execution

A technical heating main test program was developed for detecting heat losses from the heat source on the basis of the technical documentation. The test program was accepted for implementation by August 10, 2017.

Heat loss tests were conducted from September 15 through September 17, in full and in accordance with the technical and operational test programs.

At all testing stages parameters were maintained at the heat source as close to the specified values as possible:
temperature in the supply heating line:
design temperature – 87.04 ºC;
actual temperature – 85.9 ºC;

flow rate in the supply heating line:
design flow rate – 53.87 t/h;
actual flow rate – 52.91 t/h.

At the final testing stage, the water temperature at the SDPP outlet increased within forty minutes by 15.0°C. The "temperature wave" passage along the test ring was recorded at each control point.

Measurement of the heating water flow rate simultaneously in the supply and return heat pipelines, as well as feeding the heating network from the deaerator, made it possible to determine and compare the leakage rate from the test ring, which averaged 0.26 t/h; the deviation of the direct measurement of the heating network make-up flow and its calculated value determined through the difference in the heating water flow rates in the supply and return pipelines was 0.05 t/h.

Test data processing

The test data was processed as follows. For each observation point, taking into account the actual run of water between the observation points (see Table 3), determined by the "temperature wave" method, the water temperature values obtained from 20 consecutive measurements in the main test period were averaged (from 20.00 h. on 16.08.17 through 20.00 h. on 17.08.17).

The heating water flow rates in the supply and return heat lines of the test ring were averaged by the indications of flow meters.

Table 3 also contains the calculation data for actual heat losses $Q_{s.l.}$ and $Q_{r.l.}$, average annual heat losses $Q_{n.s.}^{lav.an}$ and $Q_{n.r.l.}^{av.an}$ and ratios of these heat losses to the normative ones K_s , K_r along the supply and return lines for each section of the tested ring.

The average annual heat losses at the tested network sections and the ratio of these heat losses to the normative ones were determined with an error of 4.3%.

Computational error for indicators was calculated based on the measurement results by the following formula:

$$\delta = \delta Q_{n.s.l.}^{av.an} = \delta Q_t = \delta G_{s.l.}{}^2 + \delta G_{r.l.}{}^2 + \delta \Delta^2 t = 3.0^2 + 3.0^2 + 0.28^2 = 4.3\ \%,$$

where δ - relative computational error, %; δ Qn.s.lav.an - relative error of average annual loss calculation, %; δ Qt relative error of heat loss calculation determined during tests based on the measurement results of heating water flow rate and temperature; $\delta G_{s.l.}$, $\delta G_{r.l.}$ – relative permissible error of measured heating water flow rates.

The relative error in water flow rate measurement was determined from the flow meter characteristics.

The relative error in water temperature measurement was determined by formula:

$$\delta \Delta t = 2*(\delta t)^2 = 2*(0.2)^2 = 0.28\ \%,$$

where δt – relative permissible error in temperature measurement.

Table 3: Determination of the time of water passage through the tested network sections

Section		Inner pipeline diameter di, mm	Section length, l, m	Section pipeline volume V, m^3	Water specific gravity at design temperature, *γd*, kg/m^3 *	Water specific gravity at actual test temperature, *γa*, kg/m^3 **	Design water flow rate at the section, Gd, t/h	Actual water flow rate at the section, Ga, t/h	Design time of water passage, *Td*, min	Actual time of water passage, *Ta*, min	Total expected time, Td^{Σ}, min	Total actual test time, Ta^{Σ}, min
s-n 1	SDPP - BPS	530.0	1794.0	395.8	974.35	977.92	52.9	52.9	437	439	18 h. 50 min.	18 h. 54 min.
	BPS - SDPP	530.0	1794.0	395.8	975.23	978.49	52.7	52.7	440	441		
s-n 2	BPS - HC-6	406.0	565.0	73.1	974.84	979.10	52.9	52.8	81	81		
	HC-6 - BPS	406.0	565.0	73.1	975.00	979.63	52.7	52.7	81	82		
s-n 3	HC-6 - HC-12	315.0	522.0	40.7	977.16	981.24	52.8	52.7	45	45		
	HC-12 - HC-6	315.0	522.0	40.7	981.82	983.04	52.7	52.7	46	46		

** water specific gravity is taken according to the average temperature at the beginning and end of the section in the design test mode;*

*** water specific gravity is taken according to the average actual temperature at the beginning and end of the section during the tests.*

Journal of Applied Engineering Science Vol. 17, No. 3, 2019
ISSN 1451-4117

Comparison of the test data and computational results for the mathematical model of thermal inertia of a branched district heat supply system

Thermal inertia and heating water temperature values were calculated by formulas (30-38) for a branched district heating network when dividing the heating network into 1, 10, 20 and 100 sections.

Comparison of the test data and computational results (see Fig. 2) shows that the deviation of the computational results of the model (formula 38) from the actual values lies within the measurement error range already when a network 2881 m long was divided into 20 sections. This indicates a high degree reliability of the developed model.

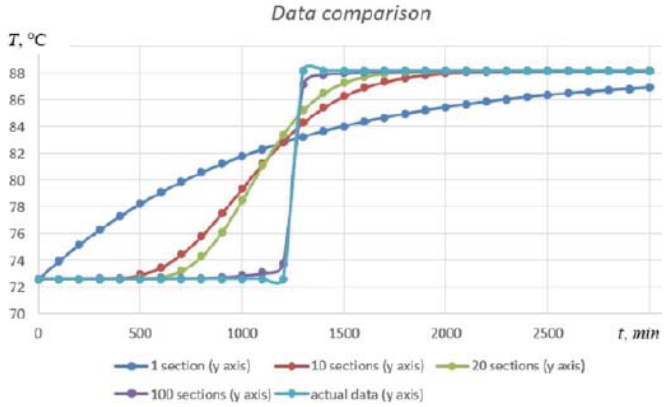

Figure 2: Comparison of the test data and computational results

To evaluate the managerial decision making method for heat delivery in district heating networks based on solving a sequence of recurrent relations of first order differential equations (formula 38), and compare it with the existing intelligent managerial decision making models, the MAPE and Accuracy coefficients were calculated using the formulas:

$$MAPE=\frac{1}{n}\sum_{i=1}^{n}\frac{|T_i'-T_i|}{T_i}\rightarrow \min \quad (39)$$

$$Accuracy=1-MAPE \rightarrow 100\% \quad (40)$$

where T'i – design temperature value calculated by formula (38); Ti – actual temperature value (see Fig. 2); n – count rate.

In the course of the analysis, the MAPE and Accuracy coefficients were calculated for the following methods: heat supply method proposed in the article, non-linear regression, generalized regression neural network (GRNN), radial basis neural network, and linear neural network.

At first, the data obtained using formula (38) and presented in Figure 2 were divided into 2 days. Then two-day nonlinear regression equations were constructed, which are presented in Figures 3 and 4.

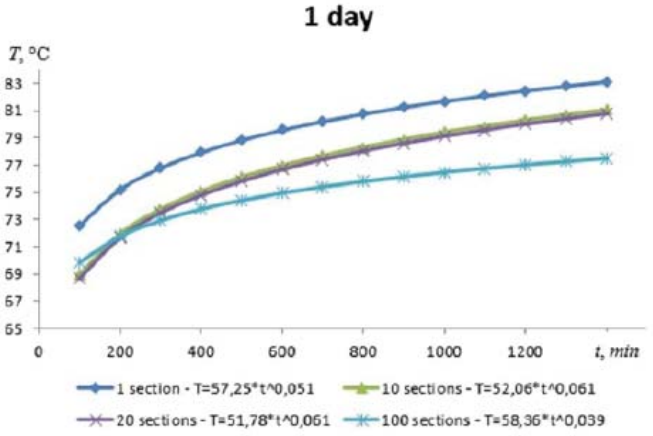

Figure 3: One-day nonlinear regression equations

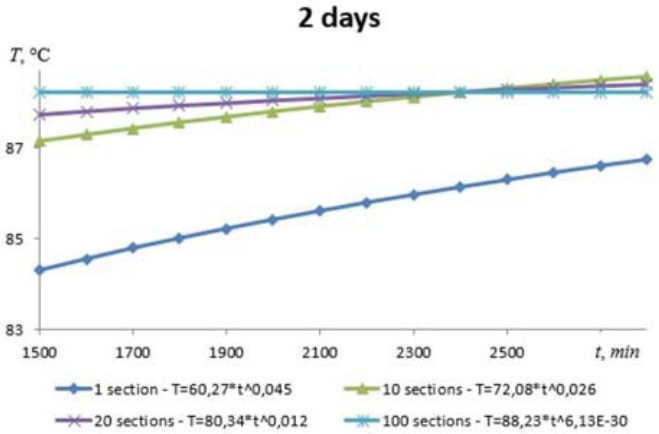

Figure 4: Two-day nonlinear regression equations

Based on the calculated nonlinear regression equations (see Fig. 3 and 4), the MAPE and Accuracy values were calculated for 2 days. The calculations are summarized in tables 4 and 5.

	1 section	10 sections	20 sections	100 sections
	Proposed model			
MAPE	5.38	2.69	2.21	0.21
Accuracy	94.62	97.31	97.79	99.79
	Nonlinear regression			
MAPE	5.49	4.41	4.32	3.46
Accuracy	94.51	95.59	95.68	96.54

Table 4: MAPE and Accuracy calculation for 1 day

	1 section	10 sections	20 sections	100 sections
	Proposed model			
MAPE	2.3	0.47	0.2	0.04
Accuracy	97.7	99.53	99.8	99.96
	Nonlinear regression			
MAPE	2.26	0.52	0.29	0.02
Accuracy	97.74	99.48	99.71	99.98

Table 5: MAPE and Accuracy calculation for 2 days

After calculating the MAPE and Accuracy values, neural models were constructed using nonlinear regression. The algorithm for constructing neural networks in the Matlab application program consists of 3 steps:

Step 1. Enter the input, output and control sample.

Sample	Parameters
Input	x = [100, 200, 300, 400, 500, 600, 700, 800, 900, 1000, 1100, 1200, 1300, 1400]
Output	y = [73.967121, 75.187203, 76.300492, 77.316335, 78.243261, 79.089054, 79.860814, 80.565022, 81.207591, 81.793916, 82.328919, 82.817094, 83.262539, 83.668995]
Control	y_k=[72.63, 72.63, 72.63, 72.63, 72.63, 72.63, 72.63, 72.63, 72.63, 72.63, 72.63, 72.63, 88.2, 88.2]

Step 2. Create the neural network.

Neural network		
generalized regression	radial basis	linear
a_1=newgrnn(x,y.0.01)	a_2=newrbe(x, y)	a_3=newlind(x, y)

The model of the created neural network is shown in Fig. 5.

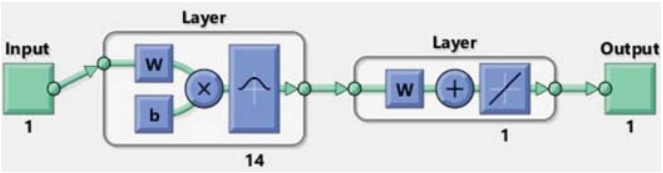

Figure 5:. General layout of the neural network

Step 3. Withdraw the results of the neural network operation

Neural network		
generalized regression	radial basis	linear

The output of the results of the neural network operation is presented in graphical form in Figure 6.

regression		
y_1 = sim(a_1, y_k)	y_2 = sim(a_2, y_k)	y_3 = sim(a_3, y_k)

After that, the MAPE and Accuracy values were calculated for three neural networks. The calculations are summarizedin table 6.

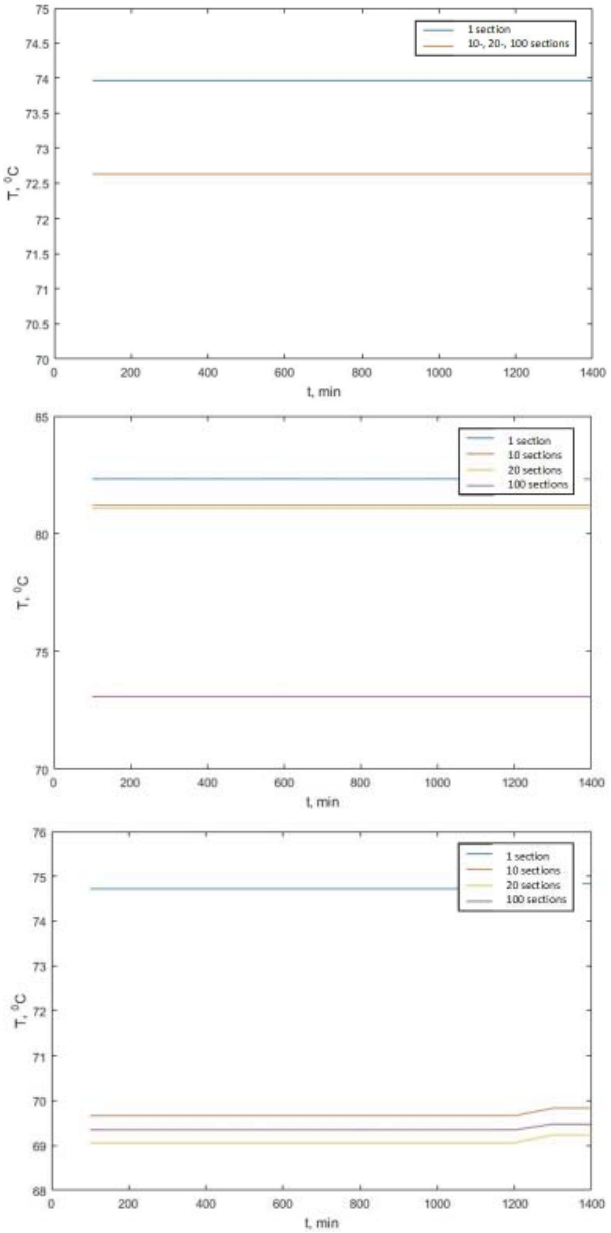

Figure 6: Neural network modelling:
a – generalized regression, b – radial basis, c – linear

Table 6: Calculation of MAPE and Accuracy values for neural models

	1 section	10 sections	20 sections	100 sections
	GRNN			
MAPE	3.01	2.14	2.14	2.14
Accuracy	96.99	97.86	97.86	97.86
	Radial basis neural network			
MAPE	7.78	7.2	7.13	2.44
Accuracy	92.22	92.8	92.87	97.56
	Linear neural network			
MAPE	3.48	5.21	5.87	5.53
Accuracy	96.52	94.79	94.13	94.47

Journal of Applied Engineering Science Vol. 17, No. 3, 2019
ISSN 1451-4117

DISCUSSION

The analysis of the averaged data given in tables 4, 5 and 6, allowed us to draw the following conclusions:

First, the proposed method has an advantage in terms of MAPE over the non-linear regression model by 1.63 times, over the radial basis neural network by 2.34 times, over the linear neural network by 1.9 times and has an advantage in terms of Accuracy over the non-linear regression model by 1.02 times, over the radial basis neural network by 1.04 times, over the linear neural network by 1.025 times.

Secondly, the proposed method has similar results with the generalized-regression neural network and is inferior to it in terms of MAPE by 0.89 times and in terms of Accuracy by 0.997 times.

Thirdly, when analyzing 100 network sections, the proposed method has an advantage over all models; in terms of MAPE over the non-linear regression model by 16.48 times, over the generalized-regression neural network by 10.19 times, over the radial basis neural network by 11.61 times, over linear neural network by 26.33 times. And it has an advantage in terms of Accuracy over the non-linear regression model by 1.03 times, over the generalized-regression neural network by 1.02 times, over the neural network of the radial basis by 1.02 times, and over the linear neural network by 1.06 times.

CONCLUSION

The paper presents a direct analytical solution of the n-dimensional system of recurrently related differential equations taking into account the initial conditions applicable to the mathematical model of thermal inertia in a branched heating system.

The obtained system of recurrently related differential equations allows for real-time forecasting of daily heat supply schedules.

Comparison of the test data and computational results shows that the deviation of the model computational results from the actual values lies within the measurement error already when a network of 2,881 m long is divided into 20 sections.

Analysis of the data for the case when the network is divided into 100 sections shows that based on the numerical values of MAPE and Accuracy indicators the proposed model has an advantage over a non-linear regression model, a generalized-regression neural model, at least by 10.19 and more times.

ACKNOWLEDGMENTS

The research was carried out within the framework of initiative scientific projects of a fundamental nature as a basic part of the state task of the Ministry of Education №13.9179.2017/8.9.

REFERENCES

1. Sokolov, E.Ya. (1963) District heating introduction and heating networks. Moscow-Leningrad: State Energy Publishing House.
2. Baykasoğlu, A., & Ozsoydan, F. B. (2018). Dynamic scheduling of parallel heat treatment furnaces: A case study at a manufacturing system. Journal of Manufacturing Systems, vol. 46, 152–162, DOI:10.1016/j.jmsy.2017.12.005
3. Yang, Ch., Chen, W., Zhao, R., & Xu, T. (2018). Stochastic analysis of effective moment of inertia of cracked in-service reinforced concrete beams. Journal of Southwest Jiaotong University, vol. 53, no. 3, 492–499, DOI: 10.3969/j.issn.0258-2724.2018.03.009.
4. Magli, S., Lodi, C., Contini, F. M., Muscio, A., & Tartarini, P. (2016). Dynamic analysis of the heat released by tertiary buildings and the effects of urban heat island mitigation strategies. Energy and Buildings, vol. 114, 164–172, DOI:10.1016/j.enbuild.2015.05.037
5. Sheng, Shiqi, and Tu, Z.C. (2013). Universality of energy conversion efficiency for optimal tight-coupling heat engines and refrigerators. Journal of Physics A: Mathematical and Theoretical vol. 46, no. 40, DOI:10.1088/1751-8113/46/40/402001.
6. Bolatturk A. (2006). Determination of optimum insulation thickness for building walls with respect to various fuels and climate zones in Turkey. Appl Therm Eng, vol. 26, no.11, 12, 1301–1309. DOI: 10.1016/j.applthermaleng.2005.10.019.
7. Kalema, T., Jóhannesson, G., Pylsy, P., Hagengran, P. (2008). Accuracy of Energy Analysis of Buildings: A Comparison of a Monthly Energy Balance Method and Simulation Methods in Calculating the Energy Consumption and the Effect of Thermal Mass, vol. 32, no 2, 101-130, DOI: 10.1177/1744259108093920.
8. Stepanov V., Starikova, N. and Stepanova, T. (2000). Indices for estimation of energy conservation in space heating. Energy and buildings, vol. 30, no.3, 189-193, DOI: 10.1016/S0378-7788(99)00013-4.
9. Valero, A. (2006). Exergy accounting: capabilities and drawbacks. Energy, vol. 31, no. 1, 164-180, DOI: 10.1016/j.energy.2004.04.054.
10. Torío, H., Angelotti, A., Schmidt, D. (2009). Exergy analysis of renewable energy-based climatisation systems for buildings: a critical view. Energy and Buildings, vol. 41, no. 3, 248-271, DOI: 10.1016/j.enbuild.2008.10.006.
11. Romero, J.C., Linares, P. (2014). Exergy as a global energy sustainability indicator. A review of the state of the art. Renewable and Sustainable Energy Reviews, vol. 33, 427-442, DOI: 10.1016/j.rser.2014.02.012.
12. Bass, M.S., Batukhtin, A.G. (2011). An Integrated Approach for Optimizing the Operation of Modern Heat Supply Systems. Thermal Engineering, vol. 58, no. 8, 678–681, DOI:10.1134/S0040601511080052

13. Goryachikh N.V., Batukhtin A.G., Ivanov 2010. S.A. Some Methods for Making Cogeneration Stations More Maneuverable. Thermal Engineering, vol. 57, no. 10, 892–896, DOI:10.1134/S0040601510100125
14. Kicsiny, R. (2014). New delay differential equation models for heating systems with pipes, Int. J. Heat Mass Transfer, vol. 79, 807–815, DOI: 10.1016/j.ijheatmasstransfer.2014.08.058.
15. Bau, U., Braatz, AL., Lanzerath, F., Herty, M., Bardow, A. (2015). Control of adsorption chillers by a gradient descent method for optimal cycle time allocation International Journal of Refrigeration - Revue Internationale Du Froid, vol. 56, 52-64, DOI: 10.1016/j.ijrefrig.2015.03.026.
16. Kicsiny, R. (2017) Grey-box model for pipe temperature based on linear regression International Journal of Heat and Mass Transfer, vol. 107, 13-20, DOI: 10.1016/j.ijheatmasstransfer.2016.11.033/
17. Messerle V.E., Karpenko E.I., Ustimenko A.B., Lavrichshev O.A. (2013). Plasma preparation of coal to combustion in power boilers. Fuel Processing Technology, vol. 107, 93–98, DOI: 10.1016/j.fuproc.2012.07.001.
18. Messerle V.E., Karpenko E.I., Ustimenko A.B. (2014). Plasma Assisted Power Coal Combustion in the Furnace of Utility Boiler: Numerical Modelling and Full-Scale Test. Fuel, vol. 126, 294-300, DOI: 10.1016/j.fuel.2014.02.047.
19. Messerle V.E., Mosse A.L., Ustimenko A.B. (2016). Municipal Solid Waste Plasma Processing: Thermodynamic Computation and Experiment. IEEE Transactions on Plasma Science, vol. 99, 1-6, DOI: 10.1109/TPS.2016.2601107
20. Messerle V.E., Ustimenko A.B., Lavrichshev O.A. (2016). Comparative study of coal plasma gasification: Simulation and experiment. Fuel, vol. 164, 172-179, DOI:10.1016/j.fuel.2015.09.095
21. Gao H., Chui E., Runstedler A. (2010). Numerical investigation of plasma ignition process in a utility boiler. Proceedings of 6th International Workshop and Exhibition on Plasma Assisted Combustion (IWEPAC). Heilbronn, Germany.
22. Karpenko E. I., Rinchinov A. P., Karpenko Y. E., Bass, M. S., Batukhtin S. G. (2016). The results of the tests of experimental-industrial plasma-cyclone installation. Industrial Energetics, vol. 4, 24-27, DOI: 10.12973/ejmste/79043
23. Kaminski, K., Krzyzynski T. (2015). Modeling and Simulation of the Solar Collector Using Different Approaches. Mechatronics: Ideas, Challenges, Solutions and Applications, 131-151, DOI: 10.1007/978-3-319-26886-6_9
24. Hussain, MI., Ali, A., Lee, GH. (2016). Multi-module concentrated photovoltaic thermal system feasibility for greenhouse heating: Model validation and techno-economic analysis. Solar Energy, vol. 135, 719-730, DOI: 10.1016/j.solener.2016.06.053.
25. Beg, O. Anwar; Ali, Nasir; Zaman, Akbar. (2016). Computational modeling of heat transfer in an annular porous medium solar energy absorber with the P1-radiative differential approximation. Journal of the Taiwan Institute of Chemical Engineers, vol. 66, 258-268, DOI: 10.1016/j.jtice.2016.06.034
26. Li, H. and Chen, Zh. (2008). Overview of different wind generator systems and their comparisons. IET Renewable Power Generation, vol. 2, no. 2, 123-138, DOI: 10.1049/iet-rpg:20070044
27. Smith, E., Koolnapadol, N., Promvonge, P. (2012). Heat transfer behavior in a square duct with tandem wire coil element insert. ChinJChem Eng, vol. 20, 863–869, WOS:000311472200008
28. Thianpong, C., Yongsiri, K., Nanan, K. and Eiamsa-ard, S. (2012). Thermal performance evaluation of heat exchangers fitted with twisted-ring turbulators. IntCommun Heat Mass Transf, vol. 39, 861–868, DOI: 10.1016/j.icheatmasstransfer.2012.04.004
29. Kicsiny, R. (2016). Improved multiple linear regression based models for solar collectors. Renewable Energy, vol. 91, 224–232, DOI: 10.1016/j.renene.2016.01.056.
30. Stevanovic, V.D., B. Zivkovic, S. Prica, B. Maslovaric, V. Karamarkovic, V. Trkulja, (2009). Prediction of thermal transients in district heating systems. Energy Convers. Manage, vol. 50, 2167–2173, DOI: 10.1016/j.enconman.2009.04.034
31. Polyanin, A.D., Zaitsev, V.F. (2003). Handbook of Exact Solutions for Ordinary Differential Equations, 2nd Edition, Chapman & Hall/CRC, Boca Raton.
32. Karpenko E.I., Trusov B.G. (1995). A Comparative Analysis of Plasma and Fire Technologies of Pulverized Coal Ignition, Combustion and Gasification Using a Mathematical Model of chemically nonequilibrum system. Thermophysics and Aeromechanics, vol. 2, no. 23, p. 245-250.
33. Saleh, A.M., Mueller, D.W., Abu-Mulaweh, H.I. (2015). Flat-Plate Solar Collector in Transient Operation: Modeling and Measurements. Journal of Thermal Science and Engineering Applications, vol. 7, DOI: 10.1115/1.4028569
34. Etter, D.M., Kuncicky, D., Moore, H. (2004). Introduction to MATLAB 7, Springer.
35. Khelifa, A., Touafek, K., Ben Moussa, H., Tabet, I. (2016). Modeling and detailed study of hybrid photovoltaic thermal (PV/T) solar collector. Solar Energy, vol. 135, 169-176, DOI: 10.1016/j.solener.2016.05.048.
36. Gholampour, M., Ameri, M. (2015). Design Considerations of Photovoltaic/Thermal Air Systems: Energetic and Exergetic Approaches. Journal of Solar Energy Engineering-Transactions of the ASME, vol. 137 (031005), DOI: 10.1115/1.4029107
37. Khelifa, A., Touafek, K., Ben M. (2015). Approach for the modelling of hybrid photovoltaic-thermal solar collector. IET Renewable Power Generation, vol. 9, 207-217, DOI: 10.1049/iet-rpg.2014.0076.

38. Batukhtin A. (2017). Solving a Sequence of Recurrence Relations for First-Order Differential Equations. Eurasia Journal of Mathematics, Science and Technology Education, vol. 13, no 11, 7179-7191, DOI: 10.12973/ejmste/79043
39. Wang, D., Zhi, Y., Jia, H., Hou, K., Zhang. (2019). Optimal scheduling strategy of district integrated heat and power system with wind power and multiple energy stations considering thermal inertia of buildings under different heating regulation modes. Applied Energy, 341–358, DOI: 10.1016/j.apenergy.2019.01.199
40. Kim, Z., Shin, Y., Yu, J., Kim, G., & Hwang, S. (2019). Development of NOx removal process for LNG evaporation system: Comparative assessment between response surface methodology (RSM) and artificial neural network (ANN). Journal of Industrial and Engineering Chemistry, vol. 74, 136–147, DOI10.1016/j.jiec.2019.02.020
41. Gonzalez, P.A., Zamarreno, J.A. (2005). Prediction of hourly energy consumption in buildings based on a feedback artificial neural network. Energ. Build., vol. 37, no 6, p. 595-601.

Paper submitted: 09.06.2019.
Paper accepted: 29.07.2019.